Cosmic-ray mass composition study and ultra-high-energy neutrino search with the Telescope Array experiment data

Yana Zhezher

ICRR, 2019

Overview

1. Ultra-high-energy cosmic-ray mass composition study with the Telescope Array surface detector data
2. Determination of a lower limit on the ultrahigh-energy proton-to-helium ratio from the measurements the X_{max} distribution
3. Ultra-high-energy neutrino search with the Telescope Array surface detector data

Open issues in UHECR physics:

1. UHECR sources, UHECR production processes: "bottom-up" vs "top-down" models
2. UHECR acceleration mechanisms, possible acceleration sites
3. UHECR propagation: medium parameters, magnetic field structure, etc.

Introduction: observation of UHECR

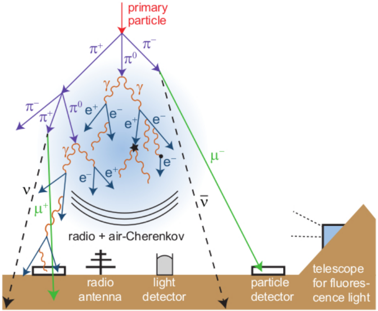

- Fluorescence light: air molecules excitation during the propagation of an EAS.
- Registration of particle distribution at the ground.
- Radio-emission caused by the propagation of the EM component of a shower.

Introduction: the Telescope Array experiment

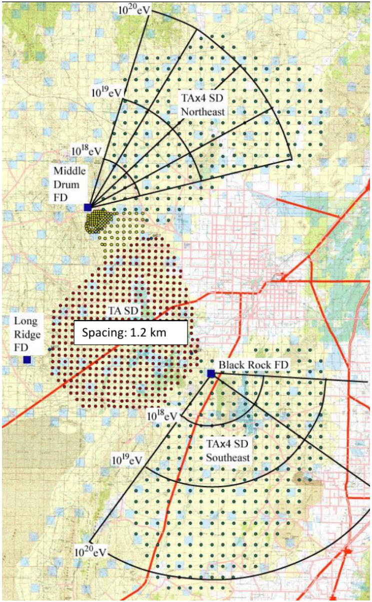

- Utah, USA
- 507 surface detectors, $S = 3$ m^2, 1.2 km distance
- 3 fluorescence detectors
- $>$ 10 years of operation

Telescope Array surface detector

< Surface Detector >

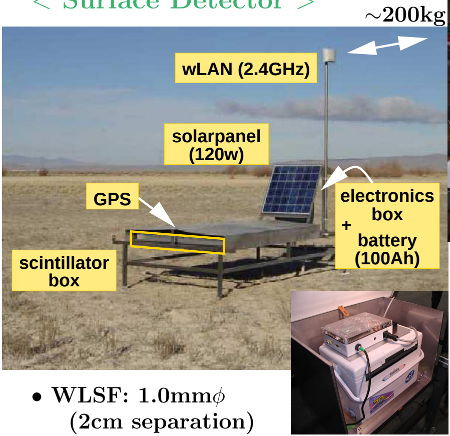

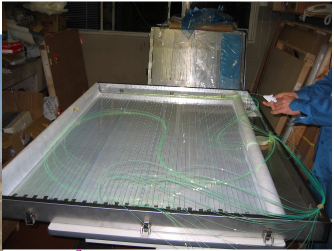

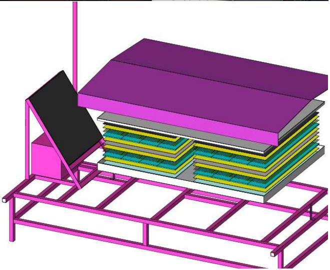

- **WLSF: 1.0mmϕ (2cm separation)**
- **PMTs: ET 9123SA $\times$ 2**
- **3m^2 (12mm $\times$ 2 layers)**

Part 1: UHECR mass composition with the TA SD

Motivation:

- One can directly determine the mass composition of cosmic rays from the observed EAS.
- Mass composition is directly connected with the UHECR acceleration mechanisms, accelerator density in the Universe and with the CR propagation processes.
- Mass composition of UHECR is the main source of uncertainties in the expected flux of cosmogenic photons and neutrinos. UHECR mass is important in the precise tests of Lorentz-invariance violation.

UHECR mass composition $\gtrsim 10^{18}$ eV

Experiment	Detector	Observables
HiRes	fluorescence stereo	X_{MAX}
Pierre Auger	fluorescence + SD (hybrid)	X_{MAX}
Telescope Array	stereo	X_{MAX}
Telescope Array	hybrid	X_{MAX}
Yakutsk	muon	ρ_μ
Pierre Auger	SD	X^{μ}_{MAX}
Pierre Auger	SD	risetime asymmetry

X_{MAX} – depth of shower maximum
X^{μ}_{MAX} – depth of muon component development
risetime – time from 10% to 50% for the total integrated signal

Mass composition study with the TA SD

p-Fe classifier (BDT)

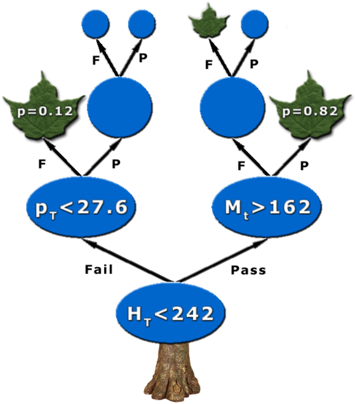

$$(a, AoP, \dots) \to \xi$$

SD detector array: > 90 % duty cycle, larger data statistics compared to FD

Comparison of ξ distributions for data with Monte-Carlo modelling

$$\Downarrow$$

$$\langle \ln A \rangle (E)$$

TA, Phys. Rev. D 99, 022002 (2019)

Boosted decision trees (shortly)

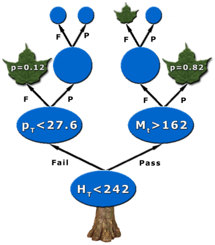

1. Find a splitting value for an observable, which gives the best separation: mostly signal events in one branch, mostly background in the other;
2. Repeat step 1 recursively, may use a new observable or re-use the same one;
3. Iterate until the stopping criterion is reached. Terminate node – "leaf";
4. Boosting: use a number of weak classifiers to build a strong one ("forest").

Observables, sensitive to the primary composition

Shower front

- Linsley curvature parameter
- Area-over-peak
- Area-over-peak slope
- Number of detectors, excluded from the shower front approximation during event reconstruction

LDF

- S_b
- Sum of signals from all detectors of the event
- Number of detectors hit
- $\chi^2/d.o.f.$ for LDF approximations

Muons

- Full number of peaks in all FADC traces of the event
- Number of peaks in the detector with the largest signal
- Asymmetry between upper and lower layers of the detector
- Number of peaks, present only in the upper layer of the detectors
- Number of peaks, present only in the lower layer of the detectors

+ zenith angle, energy of the event

Dataset

- 9-year TA SD dataset:

  2008-05-11 — 2017-05-11

  Quality cuts:

  1. event includes 7 or more triggered stations;
  2. zenith angle is below $45°$;
  3. reconstructed core position inside the array with the distance of at least 1200 m from the edge of the array;
  4. $\chi^2/d.o.f.$ doesn't exceed 4 for both the geometry and the LDF fits;
  5. $\chi^2/d.o.f.$ doesn't exceed 5 for the joint geometry and LDF fit.
  6. an arrival direction is reconstructed with accuracy less than $5°$;
  7. fractional uncertainty of the S_{800} is less than 25 %.

  18077 events

Monte-Carlo sets

p, He, N and Fe Monte-Carlo sets with QGSJETII-03

Note: MC-sets are split into three parts with equal statistics: (I) for classifier training, (II) to calculate fractions of protons and iron nuclei, (III) for $\langle \ln A \rangle$ bias correction.

$\langle \ln A \rangle$ first estimate

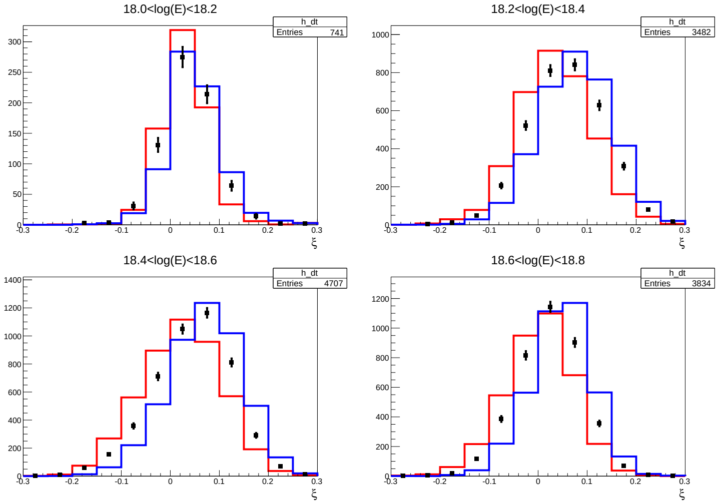

proton, iron, data

$$\langle \ln A \rangle^{(1)} = \epsilon_p \times \ln \left(M_p \right) + \epsilon_{Fe} \times \ln \left(M_{Fe} \right)$$

$\langle \ln A \rangle$ first estimate

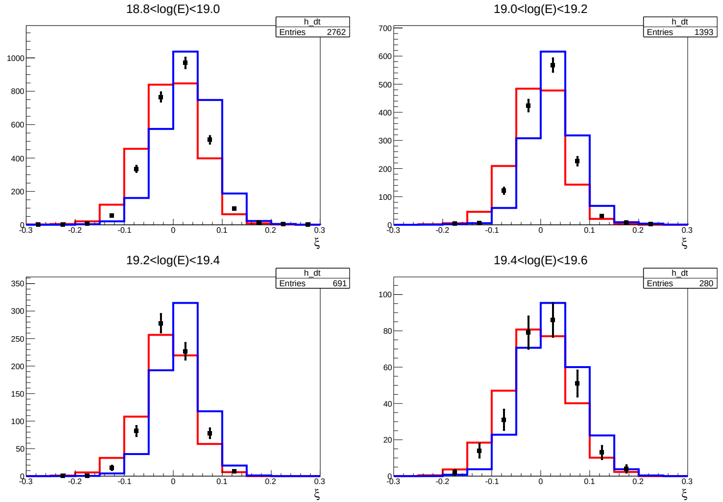

proton, iron, data

$$\langle \ln A \rangle^{(1)} = \epsilon_p \times \ln(M_p) + \epsilon_{Fe} \times \ln(M_{Fe})$$

$\langle \ln A \rangle$ bias correction

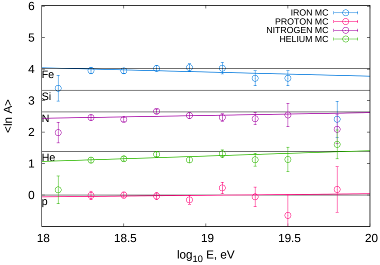

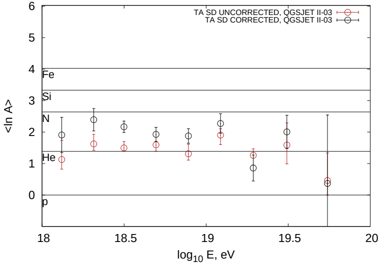

Assume that CR flux is monochromatic. In each energy bin, $\ln A_{true}$ $(\langle \ln A \rangle)$ is constructed, which relates derived masses with "true" MC ones.

Hadronic model uncertainty

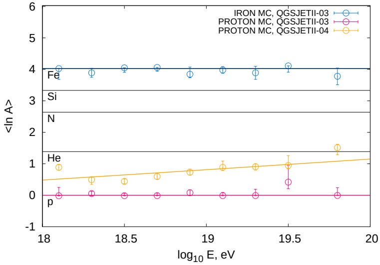

- All contemporary hadronic interaction models are phenomenological and use approximations.
- EAS muon excess problem: hadronic interaction models fail to correctly describe experimental data.
- Comparison of QGSJETII-03 и QGSJETII-04: $\delta \ln A_{hadr.} = 0.4$.

TA SD composition results

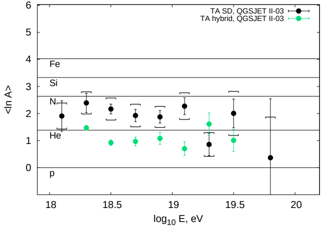

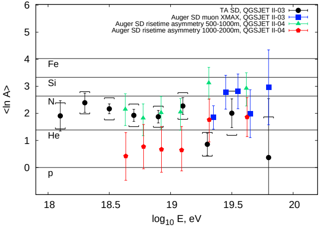

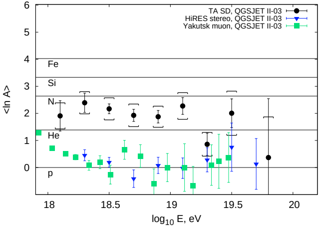

$$\langle \ln A \rangle = 2.0 \pm 0.1(stat.) \pm 0.44(syst.)$$

R. U. Abbasi et al. [Telescope Array Collaboration]. PRD, 2019

Part 1: moving beyond

How to improve the analysis:

1. Better discrimination between primary particles.
2. Do not rely on "synthetic" variables (primary assumptions such as predefined functions, etc.).

Part 1: moving beyond

How to improve the analysis:

1. Better discrimination between primary particles.
2. Do not rely on "synthetic" variables (primary assumptions such as predefined functions, etc.).

- Instead: use "raw" observables, i.e. the time-resolved signals from detectors participating in the event.
- Method: Artificial neural networks (NN).
  - Can describe any continuous function of input data.
  - Can be tuned using examples generated using Monte-Carlo.

SD event: grid of 4×4 detectors with two separate signals for two layers each containing max. 256 points (total dim.: $4 \times 4 \times 256 \times 2$).

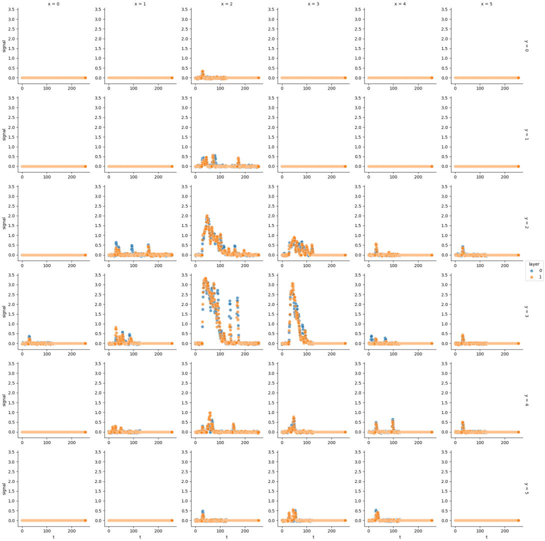

Analysis using convolutional neural networks, widely used in image and sequence processing.
NN architecture (PoS(ICRC2019)304):

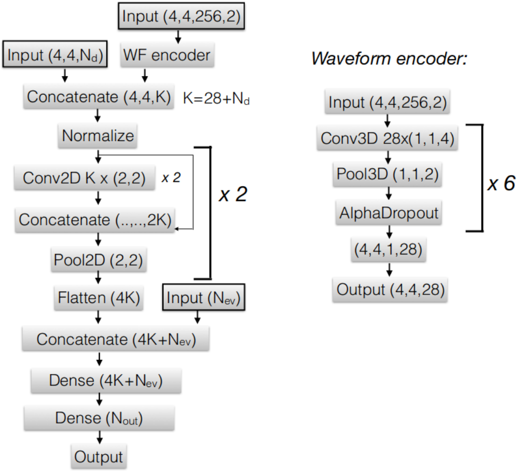

Part 1: moving beyond

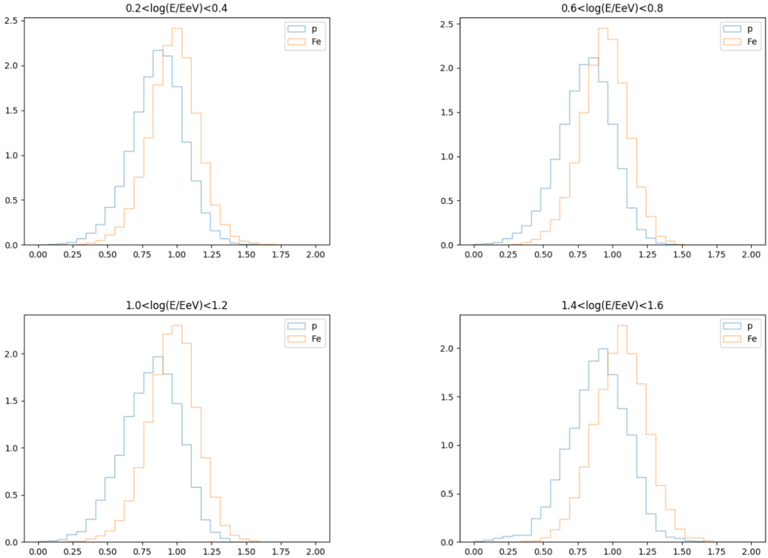

NN preliminary result: separation between primaries improved.

Part 1: moving beyond

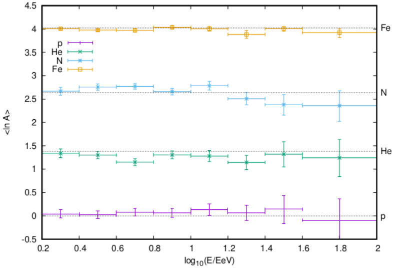

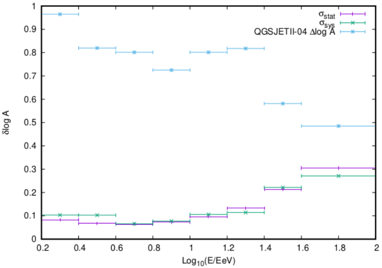

NN preliminary result: statistical and systematic uncertainties reduced.

Part 2: **p/He** ratio from the tail of X_{max} distribution

Motivation:

- UHECR mass-composition-related characteristic, derived independently;
- Constraints on cosmic-ray source models;
- Investigations of future collider safety.

Tail of $X_{\max}$ distribution

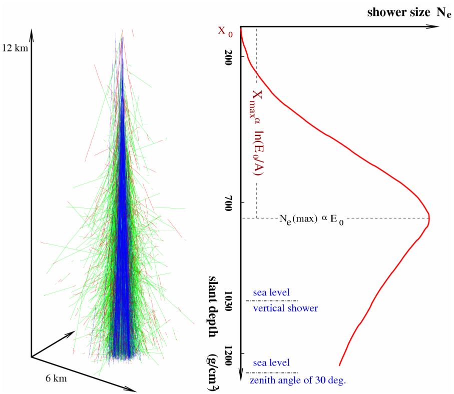

$X_{\max}$ dsitribution tail may be used independently: $\exp(-X_{\max}/\Lambda)$, where Λ – attenuation length.

Λ is sensitive to the proton-air cross-section and to the proton-to-helium ratio p/He.

Lower limit on **p/He**: methodology

1. MC sets for EAS initiated by pripary protons, helium and carbon nuclei with different hadronic interaction models.
2. Calculate Λ_i values for different mixtures of primary elements.
3. Compare Λ_i with experimental data.

Experimental Λ

Pierre Auger observatory: $10^{18.0}$ eV $< E < 10^{18.5}$eV
$\Lambda = 57.4 \pm 1.8_{stat.} \pm 1.6_{syst.}$ g/cm^2

(R. Ulrich. PoS(ICRC2015). – 2016. – № 401.)

Telescope Array experiment: $10^{18.3}$ eV $< E < 10^{19.3}$ eV
$\Lambda = 50.47 \pm 6.26$ g/cm^2

(R. U. Abbasi et al. [Telescope Array Collaboration]. Phys. Rev. D – V. 92. – № 3. – P. 032007.)

Monte-Carlo sets

Monte-Carlo sets with QGSJETII-04 and EPOS-LHC hadronic interaction models for both experiments.

Auger: 17 098 for each primary in the energy range $10^{18.0}$ eV $< E < 10^{18.5}$eV spectral index -3.293.

Telescope Array: 17 354 for each primary in the energy range from $10^{18.3}$ eV to $10^{19.3}$ eV with spectral index -3.226 for $E < 10^{18.72}$ eV and -2.66 for $E > 10^{18.72}$ eV.

$X_{\max}$ distribution (QGSJETII-04)

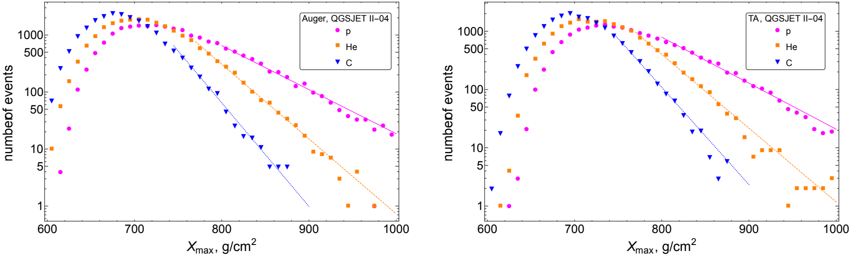

proton helium carbon

Results: p/He, Auger

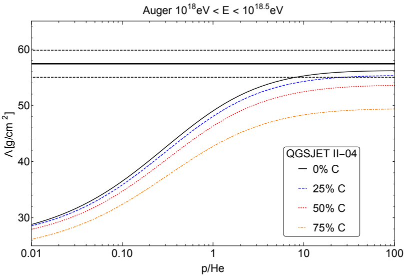

$$\text{p/He} > 7.3 \ (68\% \text{ CL}) \qquad \text{QGSJET II-04,}$$
$$\text{p/He} > 24.0 \ (68\% \text{ CL}) \qquad \text{EPOS-LHC.}$$

I. I. Karpikov, G. I. Rubtsov and Y. V. Zhezher. PRD, 2018.

Results: p/He, TA

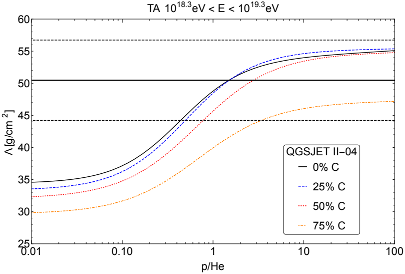

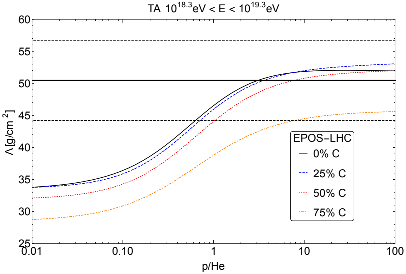

$$\mathrm{p/He} > 0.43\ (68\%\,\mathrm{CL}) \qquad \text{QGSJET II-04,}$$
$$\mathrm{p/He} > 0.63\ (68\%\,\mathrm{CL}) \qquad \text{EPOS-LHC.}$$

I. I. Karpikov, G. I. Rubtsov and Y. V. Zhezher. PRD, 2018.

Contamination by heavier elements

Proton ratio constraints w.r.t. the three-component mixture:

Auger:

$$p/(p + He + C) > 0.8 \ (68\% \, CL) \quad \text{QGSJET II-04}$$

$$p/(p + He + C) > 0.96 \ (68\% \, CL) \quad \text{EPOS-LHC.}$$

Telescope Array:

$$p/(p + He + C) > 0.20 \ (68\% \, CL) \quad \text{QGSJET II-04,}$$

$$p/(p + He + C) > 0.23 \ (68\% \, CL) \quad \text{EPOS-LHC.}$$

Part 2 conclusions

Source models

Dip model

(R. Aloisio et al., Astropart. Phys., 2007)

- Power-law injection spectrum.
- Proton primary composition.
- Uniformly-distributed sources.
- Describes the observed spectrum.
- Predicts cosmogenic photon and neutrino fluxes.

Disappointing model

(V. Berezinsky et al., Phys. Rev. D, 2006)

- Power-law injection spectrum.
- Proton composition up to $(1-3)$ eV.
- CR energy depends on charge: $E_{max}^{acc} = Z\ E_0$.
- Predicts Auger mass composition.
- Doesn't predict cosmogenic neutrinos.
- No correlation with sources due to large deflection in magnetic fields.

Part 2 conclusions

Model	Composition	Resolution
Dip model (R. Aloisio et al., Astropart. Phys., 2007)	proton	consistent
Modified dip model (R. Aloisio, V. Berezinsky, arXiv:1703.08671)	p/He = 5	excluded by Auger
Disappointing model (V. Berezinsky et al., Phys. Rev. D, 2006)	mostly proton	consistent
Helium disappointing model	helium	excluded by Auger

Part 3: UHE neutrino search with the TA SD

Motivation:

- Neutrinos are almost not absorbed during their propagation due to small cross-sections and aren't deflected in magnetic fields – pointing to the sources.
- Indication to the UHECR source types.
- Constraints on UHECR acceleration mechanisms.
- UHECR mass composition study – if primary UHECR flux is not purely protons, neutrino production is strongly suppressed.

UHE neutrino production mechanisms

1. Astrophysical neutrinos are produced in UHE hadron interactions with radiation and matter close to their astrophysical sources.
2. Cosmogenic neutrinos are born in interactions of primary protons and nuclei with background radiation during their propagation to Earth.
3. Neutrinos may be born in "top-down" models in decays of massive objects in the processes such as $D \to \nu + all$, or a possible rare decay $D \to 3\nu$.

Observation of UHE neutrino

1. "Down-going" neutrino: interaction in Earth's atmosphere through charged-current (CC) and neutral-current (NC) interactions

$$\nu_{\text{lepton}} + X \to \text{lepton} + X,$$
$$\nu_{\text{lepton}} + X \to \nu_{\text{lepton}} + X.$$

2. "Earth-skimming" neutrino: EAS invoked in the CC interactions with the minerals in the Earth's crust.
3. Radio-emission from neutrino passing through dense matter, such as ice or lunar regolith, caused by the Askaryan effect.

Down-going neutrino search with the TA SD

- Small interaction cross section -> search in highly-inclined showers (V. S. Berezinsky, G. T. Zatsepin. Phys. Lett., 1969).
- Neutrino-invoked EASes are “young” – develop deep, EM component is not absorbed.
- Time-resolved signals contain many peaks.

Down-going neutrino search with the TA SD

"young" EAS, $\theta = 19.5°$

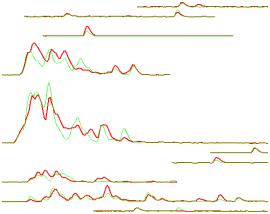

neutrino EAS (MC), $\theta = 78.6°$

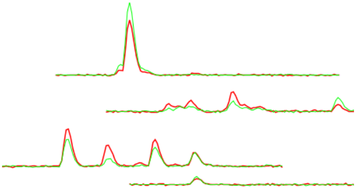

"old" EAS, 78.3°

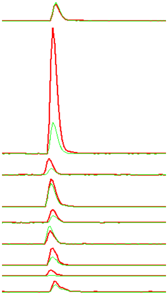

upper layer lower layer

UHE neutrino search pipeline

Neutrino-proton classifier (BDT)

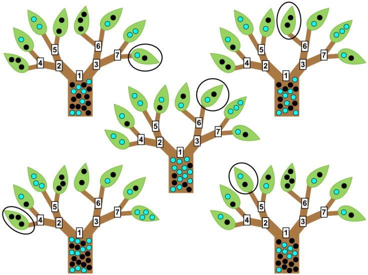

$(a, AoP, \ldots) \rightarrow \xi$

$\xi(\theta)$ distribution for Monte-Carlo sets

$\Downarrow$

ξ_{cut}

$\Downarrow$

Neutrino candidates

Dataset

- 9-year TA SD dataset:

  2008-05-11 — 2017-05-11

  Quality cuts:

  1. 5 or more triggered stations;
  2. zenith angle $\theta \in [45°; 90°]$;
  3. reconstructed core position not less than 1200 m from the boundary of the array;
  4. $\chi^2/d.o.f.$ not more than 5 for the joint approximation of shower geometry and LDF.

  197250 events

Neutrino MC

- 3000 CORSIKA shower, primary neutrino interactions with HERWIG;
- Uniform neutrino flavour flux $\nu_e : \bar{\nu}_e : \nu_\mu : \bar{\nu}_\mu : \nu_\tau : \bar{\nu}_\tau = 1 : 1 : 1 : 1 : 1 : 1$; neutrino type randomly assigned for each event;
- Energies: $3 \times 10^{17} - 3 \times 10^{20}$ эВ;
- Zenith angles: $\theta \in [0; 90°]$;
- Neutrinos don't interact in CORSIKA, point of first interaction calculated independently and fixed within CORSIKA:
  - Interaction depth: $T_{int} \sim 1/\sigma_{CC+NC}$;
  - Cross-sections: A. Cooper-Sarkar and S. Sarkar, JHEP, 2008.

Note: MC set split into three parts. (I) to train the classifier, (II) to optimize the cuts, (III) to calculate the exposure.

ξ distribution histogram

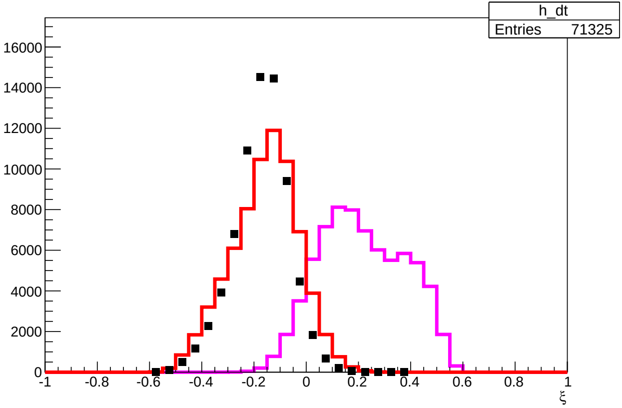

neutrino MC proton MC data

Cut optimization

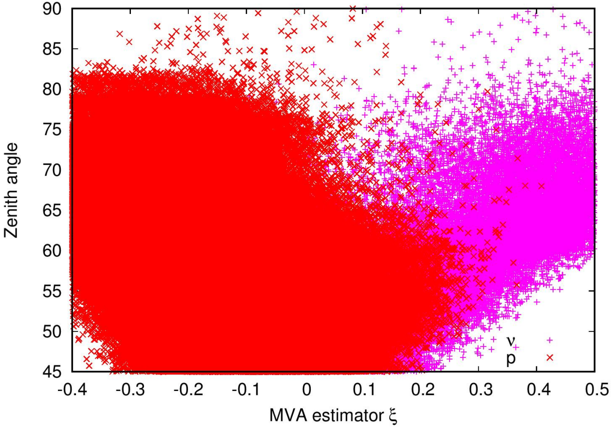

neutrino MC proton MC

Cut optimization

Neutrino candidate: $\xi > \xi_{cut}(\theta) = \xi_0 + \xi_1 \times \theta + \xi_2 \times \theta^2$.

Merit function: mean expected value of the upper limit on neutrino flux.

$\langle n_p \rangle_{90\%\ \mathrm{C.L.}}$ – upper limit on the mean value of the Poisson random variable with observed number of events n_p (Feldman-Cousins statistics).

$$f_{merit}(\xi_0, \xi_1, \xi_2, \theta) = \frac{\langle n_p \rangle_{90\%\ \mathrm{C.L.}}}{n_\nu}.$$

Cut optimization

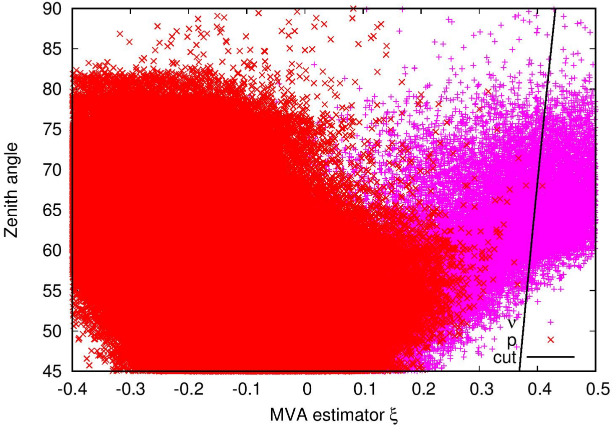

$$\xi_{cut} = 0.302 + 0.046 \times \theta - 0.006 \times \theta^2$$

neutrino MC proton MC

Exposure estimate

Geometric exposure for 9 years of observations and zenith angle range $0^\circ < \theta < 90^\circ$:

$$A^{MC}_{geom} = \int_0^{\pi/2} \sin\theta \cos\theta \; S \; T \; d\theta = 55500 \text{ km}^2 \text{ sr yr}$$

$$A^{\nu}_{eff} = A^{MC}_{geom} \times \frac{N_{pass}}{N_{thrown}} \times N_{flavor}$$

$$N_{pass} = 8278, \; N_{thrown} = 2.81 \times 10^{11}$$

$$A^{\nu}_{eff} = 1.6 \times 10^{-3} \text{ km}^2 \text{ sr yr}$$

Part 3 results

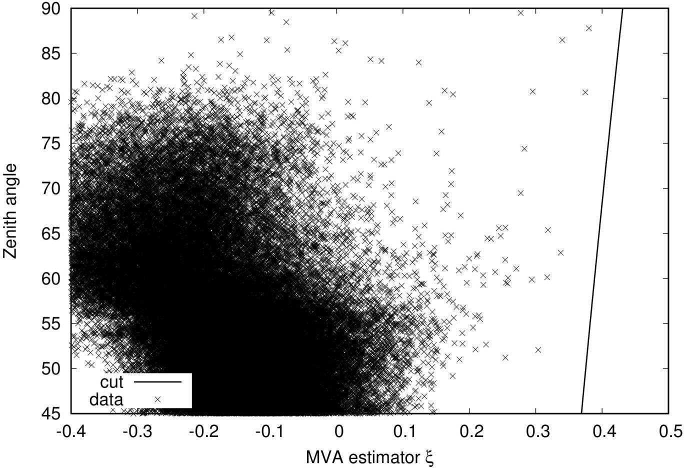

0 neutrino candidates

Part 3 results

0 neutrino candidates in dataset. Upper limit on number of neutrino events of all flavours: $\bar{n}_\nu = 2.44$ (90% C.L.).

Upper limit on diffuse flux on one-flavour neutrino for $E > 10^{18}$ eV:

$$EF_\nu < 1.58 \times 10^{-6}\ \text{GeV cm}^{-2}\ \text{s}^{-1}\ \text{sr}^{-1}\ \ (90\%\ \text{C.L.})\,.$$

Part 3 results

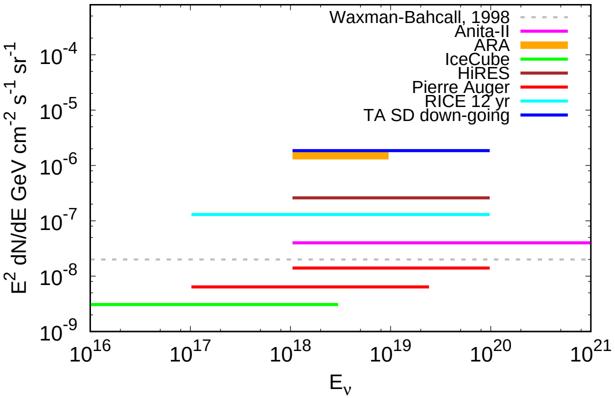

Backup

Linsley front curvature parameter

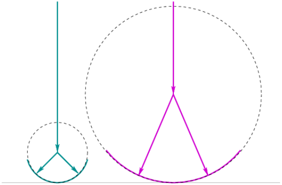

The deeper the shower develops -> the more curved front it has.

In TA, shower front is approximated as follows:

$$t_0(r) = t_0 + t_{plane} + \\ + a \times 0.67\ (1 + r/R_L)^{1.5} LDF(r)^{-0.5}$$

$$LDF(r) = S(r)/S(800\text{ m})$$

$$S(r) = \left(\frac{r}{R_m}\right)^{-1.2} \left(1 + \frac{r}{R_m}\right)^{-(\eta-1.2)} \left(1 + \frac{r^2}{R_1^2}\right)^{-0.6}$$

$$R_m = 90.0\text{ m},\ R_1 = 1000\text{ m},\ R_L = 30\text{ m}$$

$$\eta = 3.97 - 1.79(\sec(\theta) - 1)$$

$$t^i_{plane} = \frac{1}{c}\vec{n}\left(\vec{R}_i - \vec{R}_{core}\right)$$

t_{plane} – flat front arrival time

a – Linsley front curvature parameter

LDF – lateral distribution function

Area-over-peak and area-over-peak slope

- Time-resolved signal from a given station:

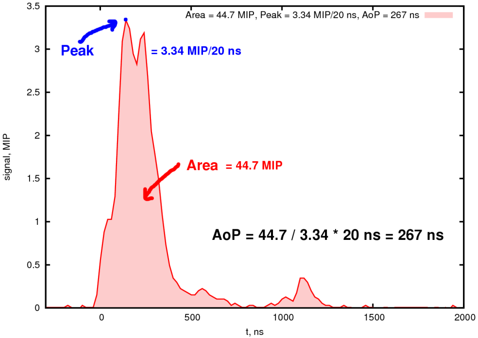

- $AoP(r)$ is approximated as follows:
  - $AoP(r) = \alpha - \beta(r/r_0 - 1.0)$
  - $r_0 = 1200\,\mathrm{m}$, α – it's value at 1200 m, β – AoP slope

S_b parameter

$$S_b = \sum_{i=1}^{N} \left[S_i \times \left(\frac{r_i}{r_0} \right)^b \right],$$

S_i – signal of i-th detector, r_i – distance to the shower core in meters, $r_0 = 1200$ m – characteristic distance. $b = 3$ and $b = 4.5$ values chosen as giving the best separation between primaries.

G. Ros, A. D. Supanitsky, G. A. Medina-Tanco et al., Astropart. Phys., 2001

Hillas plot

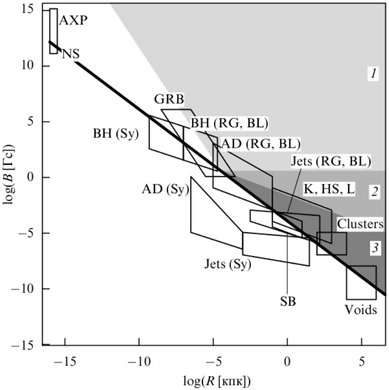

Geometric criterion:

$$R_{ac} > \frac{E}{qB}$$

K. Ptitsyna, S. Troitsky, Physics Uspekhi, 2010.

AdaBoost

Boosting – idea of making one good classifier from a number of weak ones (a forest).

- Given a weak learner, run it multiple times on (reweighted) training data.
- On each iteration: misclassified events are assigned a new weight α

$$err = \frac{N_{misidentified}}{N_{all}}, \ \alpha = \frac{1 - err}{err}.$$

- New tree with reweighted events is built and optimized. Tree weight: $TW = \ln \alpha$.
- Average over all trees with their weights:

$$y_{boost} = \frac{1}{N_{trees}} \sum \ln \alpha_i \times h_i.$$

Shower front

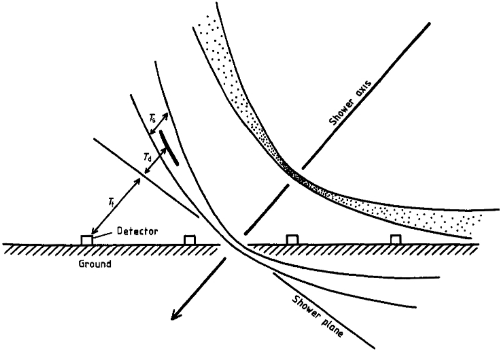

$$t_0(r) = t_0 + t_{plane} + a \times 0.67\ (1 + r/R_L)^{1.5} LDF(r)^{-0.5}$$

M. Teshima et al., J. Phys. G, 1986

Composition-sensitive observables distribution

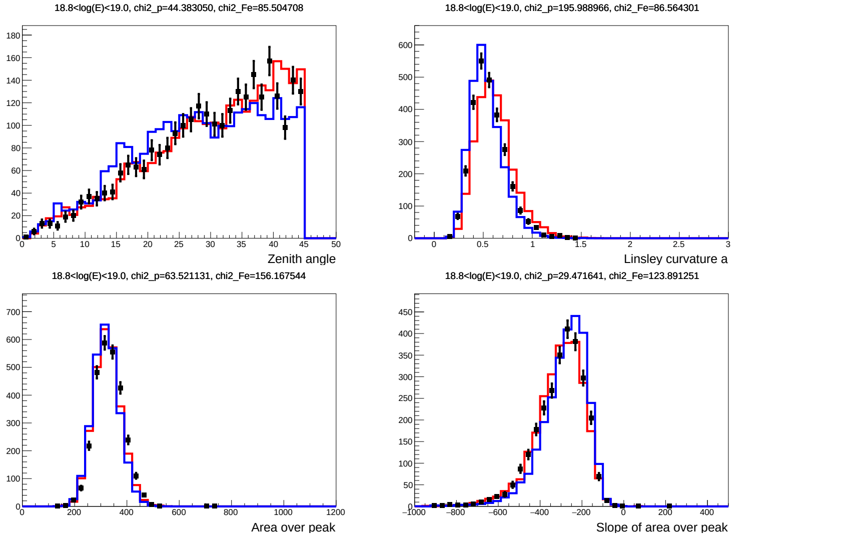

proton MC iron MC data

Composition-sensitive observables distribution

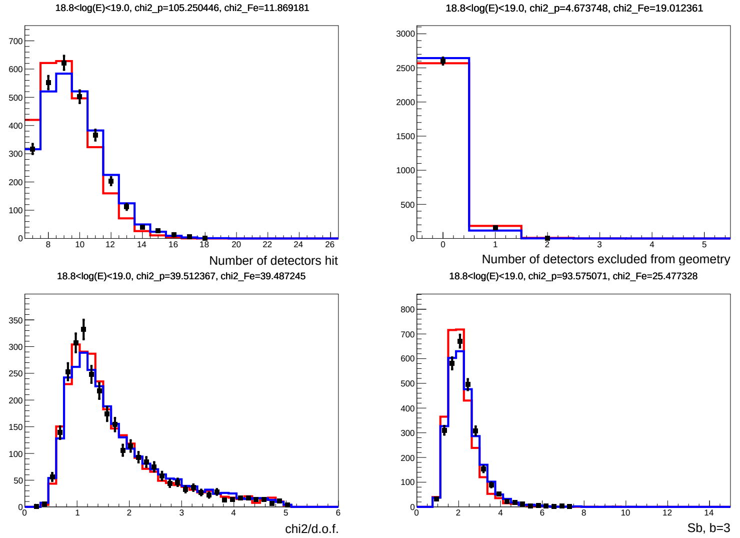

proton MC iron MC data

Composition-sensitive observables distribution

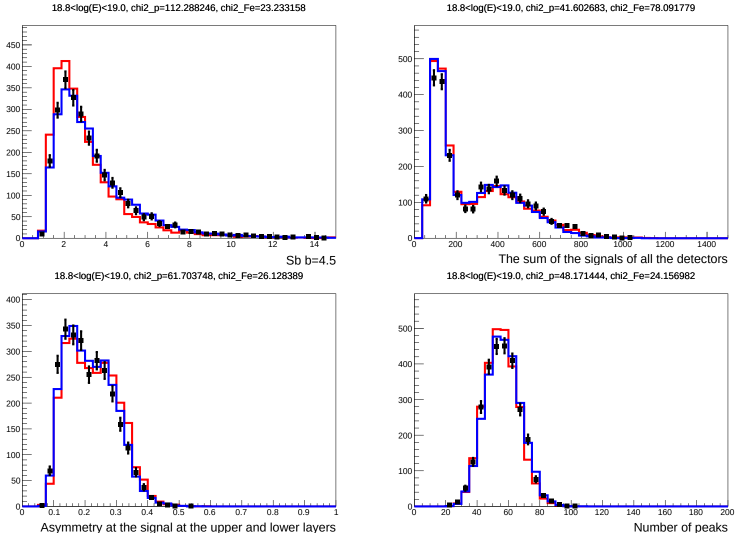

proton MC   iron MC   data

Composition-sensitive observables distribution

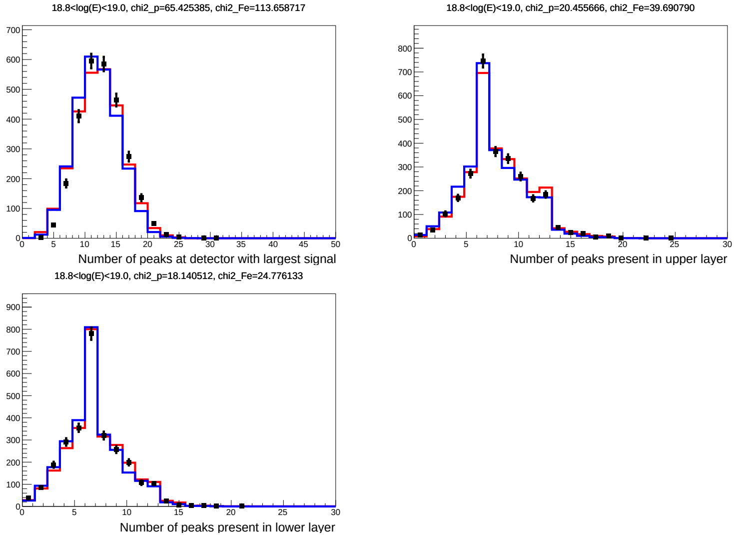

proton MC iron MC data

Dip model

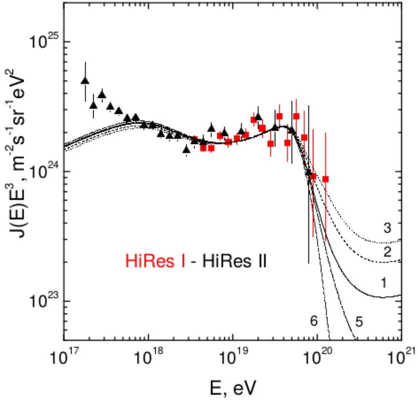

- Power-law injection spectrum.
- Proton primary composition.
- Uniformly-distributed sources.
- Describes the observed spectrum.
- Predicts cosmogenic photon and neutrino fluxes.

V. Berezinsky, A. Z. Gazizov and S. I. Grigorieva. Phys. Rev. D, 2006.

Disappointing model

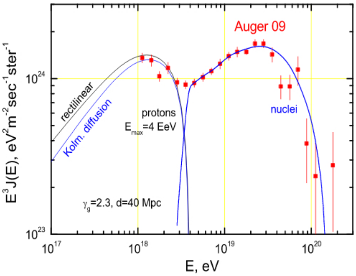

- Power-law injection spectrum.
- Proton composition up to $(1-3)$ eV.
- CR energy depends on charge: $E_{max}^{acc} = Z\ E_0$.
- Predicts Auger mass composition.
- Doesn't predict cosmogenic neutrinos.
- No correlation with sources due to large deflection in magnetic fields.

R. Aloisio, V. Berezinsky and A. Gazizov. Astropart. Phys., 2011

Askaryan effect

- EAS propagation in matter cause overabundance of electrons in it: positrons annihilate, electrons are pulled into the shower from the medium.
- Electron overabumdance $1/(Z\,E)$, doesn't depend on the medium density, up to 10 %.
- Electron overabundance creates extra radiation (Cherenkov, bremsstrahlung, transition).

G. A. Askar'yan, JETP, 1961

Number of peaks distribution

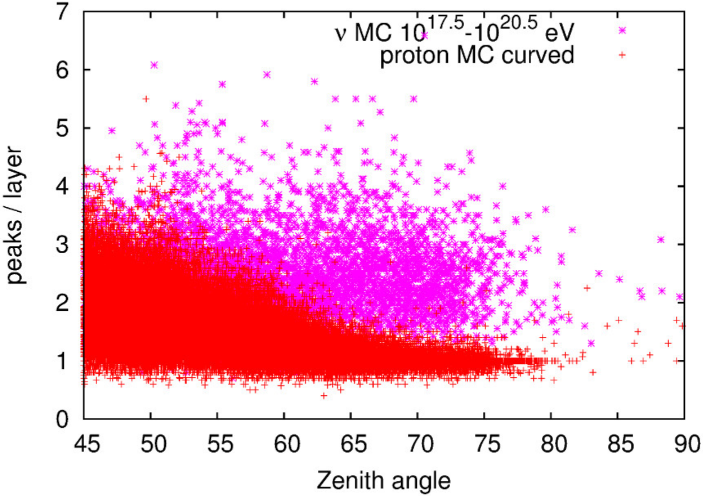

neutrino MC proton MC

ν exposure

Particle flux $J(E)$ as a function of energy:

$$J(E) = \frac{\mathrm{d}^4 N}{\mathrm{d}E\mathrm{d}A\mathrm{d}\Omega\mathrm{d}t} \simeq \frac{\Delta N_{\mathrm{sel}}(E)}{\Delta E}\frac{1}{\mathcal{E}(E)}$$

Экспозиция:

$$\mathcal{E}(E) = \int_T \int_\Omega \int_S \varepsilon(E, t, \theta, \phi, x, y)\ \cos\theta\ \mathrm{d}S\ \mathrm{d}\Omega\ \mathrm{d}t = \int_T \mathcal{A}(E, t)\ \mathrm{d}t;$$

where ε – particle registration efficiency,
$\mathcal{A}(E, t)$ – instanteneous detector aperture.

Cut optimization

- Initial values of ξ_0, ξ_1 и ξ_2 correspond to some numbers of proton and neutrino events which pass the cut n_p and n_ν.
- Surface detector exposure is proportional to n_ν.
- Number of false neutrino candidates is derived from n_p. It is a random value with Poission statistics. Since it is always a small number, one may use the Feldman-Cousins statistics.
- Number of background events is set to zero.